Available online at www.sciencedirect.com
ScienceDirect
Polymer 48 (2007) 6589–6597
polymer
www.elsevier.com/locate/polymer

Analysis of particle–solvent interactions in pH-responsive cross-linked microgel systems

B.H. Tan [a], K.C. Tam [b,*]

[a] Institute of Materials Research and Engineering, Agency for Science, Technology and Research, 3 Research Link, Singapore 117602
[b] Department of Chemical Engineering, University of Waterloo, 200 University Avenue West, Waterloo, Ontario, Canada N2L 3G1

Received 6 July 2007; received in revised form 31 August 2007; accepted 3 September 2007
Available online 7 September 2007

Abstract

Viscometry, static light scattering and turbidimetry studies were performed to investigate the interaction between pH-responsive microgels consisting of methacrylic acid (MAA) and ethyl acrylate (EA) copolymers cross-linked with di-allyl phthalate (DAP) and the solvent environment. The characteristics of microgel particles and their corresponding interaction potential were manipulated by varying the following: (a) degree of neutralization of MAA groups; α (b) salt concentrations and (c) microgel cross-linked density. Three independent interaction parameters, i.e. Huggins constant, K_h, second virial coefficient, A_2 and apparent second virial coefficient, B_{app}, which describe the degree of particle–solvent interactions, were obtained from these techniques. A scaling relationship between the three parameters given as: $B_{app}/K_h \propto \alpha \overline{M}_w A_2$ (where $\overline{M}_w$ represents the weight-average molecular weight), was proposed. Good agreement was observed, where all the data for the three different salt concentrations of each microgel with different cross-linked densities collapsed onto a single master curve. This suggested that all three techniques can accurately predict the degree of interaction between microgel particle and solvent environment. Turbidimetry, being the simplest among the three techniques is the most convenient method.

Keywords: Particle–solvent interactions; Microgels; Viscometry

1. Introduction

The colloidal phenomenon of soft particles is becoming an important field of research due to the growing interest in a variety of important systems found in biological science, such as drug delivery [1,2], water purification [3] and microfluidic devices [4]. There has been considerable progress in understanding the particle–solvent interaction of colloidal suspensions. Information on the interaction potential of these particles permits the quantitative analysis of factors governing colloidal stability [5–7]. Synthetic mono-dispersed stimuli-responsive colloids in the nano to micron size range are increasingly becoming important model systems for such studies since these particles can be prepared in a well-defined manner and with narrow size distributions [7]. Scientific knowledge on particle–solvent interaction of polymer latex systems is important since microscopic interactions between colloidal particles in polymer solutions control the flow behavior of many suspensions, which are of interest in industries that utilize colloids in their product formulations.

Recently, a number of studies to investigate the particle–solvent interaction in polymer lattices, surfactant micelles and colloidal particles have been reported [8–13]. Huglin et al. [8,9] examined cross-linked hydrogels of poly(*N*-ethylacrylamide) (PEA) in salt solutions by gravimetric method. They reported that with increasing cross-linked density, the particle–solvent interaction parameter obtained from Flory theory was enhanced [10]. Francois et al. [14] described the effect of molecular weight on the viscometric parameters of poly(4-vinylpyridine) (P4VP) polymers in ethanol solution and subsequently proposed empirical laws for $[\eta]$, K_h and A_2 as a function of molecular weights. Arleth et al. [11] compared

* Corresponding author.
E-mail address: mkctam@uwaterloo.ca (K.C. Tam).

0032-3861/$ - see front matter © 2007 Elsevier Ltd. All rights reserved.
doi:10.1016/j.polymer.2007.09.004

the osmotic second virial coefficient, A_2, measured at low concentrations from static light scattering with data determined from small angle neutron scattering (SANS) of poly(*N*-isopropylacrylamide) (PNIPAM) microgel particles as a function of temperature and discovered that the particle interactions changed across the transition temperature. At temperatures below the transition, the interactions are described by a repulsive interaction far larger than that expected for a hard sphere contact potential. Above the volume transition temperature, the potential is best described by a small, attractive interaction. The micellization phenomena in a novel biodegradable surfactant, alpha-olefin sulfonate (AOS) in mono-valent salt concentration ranging from 0 to 100 mM was studied with three independent techniques, namely dynamic light scattering, turbidity and viscosity [12,13]. With increased salt concentration, the inter-micellar attraction was observed to increase thus facilitating the formation of larger micelles with aggregation numbers exceeding 100.

In the present work, we combined data from viscometry, static light scattering and turbidimetry to investigate the interaction between pH-responsive microgels and solvent at three different salt concentrations, i.e. 10, 50 and 100 mM KCl. Model pH-responsive microgels consisting of methacrylic acid–ethyl acrylate (MAA–EA) cross-linked with di-allyl phthalate (DAP) were synthesized via the emulsion polymerization technique. The polymers are insoluble lattices at low pH. By increasing the pH, the ionization of acid groups is enhanced, which increases the solubility and osmotic pressure within the microgel, yielding interesting changes in the particle interaction potential. Three different model systems with fixed 20 mol% MAA and 80 mol% EA but varying cross-linked densities, i.e. 1, 2 and 4 wt% DAP were studied. These microgels are denoted as HASE-20-80-1, HASE-20-80-2 and HASE-20-80-4. We manipulated the characteristics of these particles and their corresponding interaction potential by varying the following: (a) degree of neutralization of MAA groups, α (b) salt concentrations, and (c) cross-linked density.

2. Experimental

2.1. Polymer synthesis

Model pH-responsive microgel particles were prepared by Dow Chemicals using the conventional semi-continuous emulsion polymerization of methacrylic acid (MAA) and ethyl acrylate (EA) cross-linked with di-allyl phthalate (DAP). The synthesis procedures were reported in our previous publications [15–19]. The polymer latexes at low pH between 1.8 and 2.5 were dialyzed in distilled deionized water using regenerated cellulose tubular membrane. The dialysis process was carried out over a one-month period, where the water was replaced weekly. This cleaning process removed all the impurities and unreacted chemicals. The chemical structure of the MAA–EA microgel series used in this study is schematically shown in Fig. 1 and the physical properties are tabulated in Table 1. These microgels are designated as HASE-*y*-*x*-*z*, where the subscripts *y* and *x* correspond to the mole percent of MAA and EA whereas *z* denotes the weight percent of cross-linker DAP. For example, the polymer with MAA/EA molar ratio of 20:80 and amount of grafted diallyl phthalate of 2 wt% is designated as HASE-20-80-2.

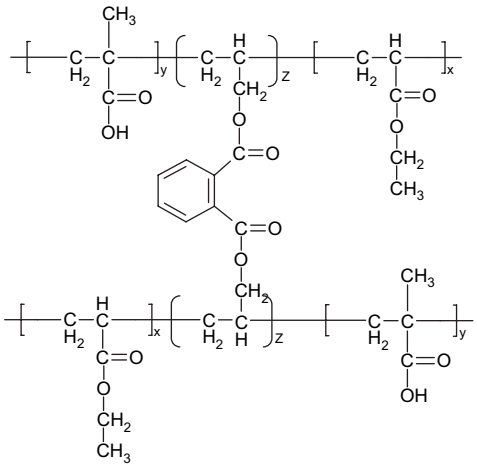

Fig. 1. Chemical structure of model cross-linked MAA–EA microgel system.

2.2. Physical characterization

The microgel suspensions were neutralized with sodium hydroxide solutions. The degree of ionization can be characterized by the degree of neutralization, α, which is the molar ratio of added base to acid groups on the microgels. Upon neutralization, the acid groups became negatively charged, which resulted in the swelling of microgels. The effects of ionic strength on the swelling behavior of our pH-responsive microgels were examined in potassium chloride KCl, where the salt concentration in the bulk solution of the microgel suspension was varied from 10 to 100 mM KCl.

2.3. Methods

2.3.1. Viscometric measurement

The dilute solution viscosity of colloids is a very important parameter that enables the characterization of the molecular dimension as well as obtaining the particle–solvent interaction parameter. The measurements were conducted using an automatic Cannon capillary viscometer at a temperature of 25 ± 0.02 °C maintained with a thermostatic environmental chamber. The efflux time was kept long (preferably more than 100 s) to minimize the need for applying kinetic corrections to the data.

The efflux time measured from the capillary viscometer was then related to the reduced and inherent viscosities by assuming that the density of the polymer solution is similar to the solvent. The formulas for the reduced and inherent viscosities are as follow:

$$\eta_{\mathrm{red}} = \frac{\eta_{\mathrm{sp}}}{c} = \frac{\eta - \eta_{\mathrm{s}}}{\eta_{\mathrm{s}} c} = \frac{t - t_{\mathrm{s}}}{t_{\mathrm{s}} c} \tag{1}$$

where η_{red} is the reduced viscosity, η_{inh} the inherent viscosity, η_{sp} the specific viscosity defined as $(\eta - \eta_{\mathrm{s}})/\eta_{\mathrm{s}}$, c the solution

Table 1
Physical properties of model pH-responsive cross-linked MAA–EA microgel systems

Microgel system	MAA/EA molar ratio (%)	DAP (wt%)	pH	R_h (α=0) (nm)	Solid content (wt%)	Polydispersity index M_w/M_n
HASE-20-80-1	20:80	1.0	1.84	36.5	9.91	1.27
HASE-20-80-2	20:80	2.0	2.24	39.8	9.90	1.25
HASE-20-80-4	20:80	4.0	1.80	41.1	9.88	1.21

concentration, η the polymer solution viscosity, η_0 the solvent viscosity, η_r the relative viscosity defined as (η/η_s), t the efflux time of the polymer solution and t_s the efflux time of the solvent.

When the solution concentration approaches zero, both the reduced and inherent viscosities approach the intrinsic viscosity:

$$[\eta] = \lim_{c\to 0} \frac{\eta_{sp}}{c} = \lim_{c\to 0} \frac{\ln \eta_r}{c} \tag{2}$$

The intrinsic viscosity, $[\eta]$, which for suspensions is the dilute limit of the viscosity increment per unit particle volume fraction, divided by the solvent viscosity. It describes the ability of the polymer molecules to increase the viscosity of the solvent in the absence of any inter-molecular interactions. The intrinsic viscosity $[\eta]$ was obtained by extrapolating the reduced and inherent viscosity data to zero polymer concentration using Huggins and Kraemer equations. The Huggins equation is represented as [20]:

$$\left(\eta_{sp}/c\right) = [\eta] + K_h[\eta]^2 c \tag{3}$$

where K_h is Huggins coefficient; a constant for a series of polymer of different molecular weights in a given solvent and temperature. The Kraemer equation is [21]:

$$(\ln \eta_r/c) = [\eta] + K_k[\eta]^2 c \tag{4}$$

where K_k is the Kraemer coefficient and theoretically, $K_h - K_k = 0.5$.

The interaction parameter of interest here is Huggins constant, K_h, which describes the particle–solvent interaction. In a theta (θ) solvent, which marks the boundary between a good and bad solvent, K_h is close to 0.5. In θ solvent, the medium provides an exact compensation for the excluded volume effect. In a ''good'' solvent, one that shows a zero or negative heat of mixing with the polymer, the molecule is in its extended conformation, and the intrinsic viscosity is high. Huggins constant, K_h is less than 0.5, where it represents strong particle–solvent interaction. In a ''poor'' solvent, one that shows a positive heat of mixing, segments of a polymer molecule attract each other more strongly than the surrounding solvent molecules. The polymer molecule assumes a more compact configuration, and the solution has a lower intrinsic viscosity. Huggins constant, K_h is greater than 0.5 in ''poor'' solvents and it represents weak particle–solvent interaction [10]. The Huggins constant is molecular-weight dependent for polymers that associates easily in solution, by either ionic or polar interactions [14,22].

2.3.2. Static light scattering

Static light scattering (SLS) was used to measure and analyze the time-average scattered intensities. This method is often used to determine microscopic properties of particles such as the z-average radius of gyration (R_g), the weight-average molecular weight ($\overline{M}_w$), and the second virial coefficient (A_2) according to Eq. (5) [23,24]:

$$\frac{Kc}{R_\theta} = \frac{1}{M_w}\left[1 + \frac{16\pi^2 n^2 \left\langle R_g^2 \right\rangle \sin^2\left(\frac{\theta}{2}\right)}{3\lambda^2}\right] + 2A_2 c \tag{5}$$

where, the Rayleigh ratio, $R_\theta = (I_s r^2/I_t \sin\theta)$; $K = [4\pi^2 n^2 (dn/dc)^2/(N_A\lambda^4)]$; c is the concentration of the polymer solution; n is the refractive index of the solvent; θ is the angle of measurement; λ is the wavelength of laser light; and N_A is Avogadro's constant. The refractive index increment of the polymer solution (dn/dc) was measured using a differential refractometer where the value obtained was ~0.1 ml/g for all the microgel solutions. A plot of (Kc/R_θ) versus $[\sin^2(\theta/2) + kc]$ (where k is a plotting constant) can be used to determine the molecular parameters. By extrapolating the data to zero angles and concentrations, R_g and A_2 can be obtained from the slopes, respectively. A simultaneous extrapolation to zero angle and concentration yields an intercept, which is the inverse of $\overline{M}_w$. The second virial coefficient, A_2 is the interaction parameter, which describes the degree of interaction between the colloid and solvent. For high molecular weight microgels ($M_w > 10^5$ g/mol), the second virial coefficient, A_2, is nearly independent of molecular weight [25]. A Brookhaven BIS200 laser scattering was used to perform the dynamic light scattering experiments at 25 ± 0.02 °C. The light source is a power adjustable vertically polarized 350 mW argon laser with a wavelength of 488 nm.

2.3.3. Turbidimetric measurement

It was reported recently that turbidimetry is a suitable technique for studying particle–solvent interaction in colloidal suspensions [26–30]. The data analysis for this method was reported in detail in our previous publication [19]. The integrated structure factor, $Z(\lambda^2,c)$ can be rewritten as:

$$Z\left(\lambda^2, c\right) = \frac{(\tau/c)}{(\tau/c)_{c=0}} \tag{6}$$

where τ is the turbidity, c the mass concentration and the subscript 0 denotes property of the microgel at $c \to 0$. Eq. (6) suggests that $Z(\lambda^2,c)$ can be calculated from a plot of (τ/c) as a function of c at fixed λ when the concentration is extrapolated to zero. In the limit of very small concentrations $Z(\lambda^2,c)$ may be approximated by:

$$Z\left(\lambda^2,c\right)^{-1} \approx 1 + 2B_{\text{app}}c \tag{7}$$

where the apparent second virial coefficient, B_{app}, represents particle–solvent interaction and is dependent on the wavelength [19]. A plot of $Z(\lambda^2,c)$ as a function of c was performed, and the slope represents B_{app}. The total scattering intensity and turbidity measurements are complimentary techniques, and under appropriate measurement conditions, these methods provide identical information on the scattering object. The classical Debye equation relates the two as described by Eq. (8) [12,31]:

$$\frac{Kc}{R_\theta} = \frac{1}{M} + 2A_2c = \frac{1}{M} + 2B_{\text{app}}c \tag{8}$$

for particle size less than the wavelength, λ, of the excitation source used in the experiment.

Measurements of transmittance between wavelength of 500 and 900 nm were conducted using a Hewlett Packard UV–Visible Spectrometer at 25 ± 0.02 °C. Initial measurements were done using cuvettes with optical path lengths of 0.2, 0.5 and 1 cm to confirm the Beer–Lambert law. Only data with transmissions of between 0.03 and 0.95 were found to be sufficiently accurate. In all cases, the turbidity was found to be independent of the optical path length within experimental errors. Within the limit of Beer–Lambert law, the determination of τ is not affected by multiple or forward scatterings. All subsequent measurements were done with cuvette of 1-cm path length.

3. Results and discussion

3.1. Swelling behavior

The pH-responsive microgel particles with varying cross-linked densities (HASE-20-80-1, HASE-20-80-2 and HASE-20-80-4) were characterized in the dilute solution regime (0.1 wt%) using the Brookhaven dynamic light scattering (DLS) system for neutralization degree (α) ranging from 0 to 1.0 and in salt concentration ranging from 10 to 100 mM KCl. In their unneutralized state, the particles were in a collapsed state with a hydrodynamic radius, R_h of ~35 nm. The pH-dependent hydrodynamic radius, R_h, showed a continuous increase as α increased from 0 to 1.0, representing the steady expansion of particles due to enhanced osmotic pressure exerted by counter-ions trapped inside the polymeric network. Swelling was reduced with increasing ionic strength and cross-linked density [15–18].

3.2. Particle–solvent interaction from viscometry measurement

Viscometric measurements using Ubbelohde viscometer were conducted on three microgels prepared in 10 mM KCl solution and at varying degree of neutralization, α. In addition, the effect of salt concentration on the particle–solvent interaction was investigated using HASE-20-80-2 microgel at varying degree of neutralization. Huggins and Kraemer equations described by Eqs. (3) and (4), respectively, were applied to all the data to determine the intrinsic viscosity $[\eta]$ and particle–solvent interaction parameter, K_h. An example is shown in Fig. 2, which displays the reduced viscosity (η_{sp}/c) and inherent viscosity $(\ln \eta_r/c)$ data as a function of microgel concentration, c, of fully neutralized microgel HASE-20-80-2 in 10 and 50 mM KCl. The solid and dotted lines represent the extrapolation of reduced and inherent viscosity data to zero polymer concentration using Eqs. (3) and (4) to yield $[\eta]$ and K_h.

Fig. 3a shows the relationship between the intrinsic viscosity, $[\eta]$, as a function of α of HASE-20-80-2 at three different salt concentrations. The intrinsic viscosity increased with α, but decreased with salt concentration. For example, $[\eta]$ for fully neutralized ($\alpha = 1$) microgel in 10 mM KCl is ~5.5 dl/g, compared to ~4.5 dl/g for microgel in 100 mM KCl. The counter-ions (K^+) from salt act as electrostatic shield between COO^- anions along the polymer backbone. The shielding effect reduced the electrostatic repulsion on the polymer backbone, leading to a reduction in the molecular coil size and a lower intrinsic viscosity. The effect of microgel cross-linked density was also investigated as depicted in Fig. 3b, where the intrinsic viscosity of microgel in 10 mM KCl solution decreased with increasing cross-linked density for a fixed α. Increasing the cross-linked density from 1 to 4 wt% DAP reduced the swelling of microgel, leading to a lower intrinsic viscosity.

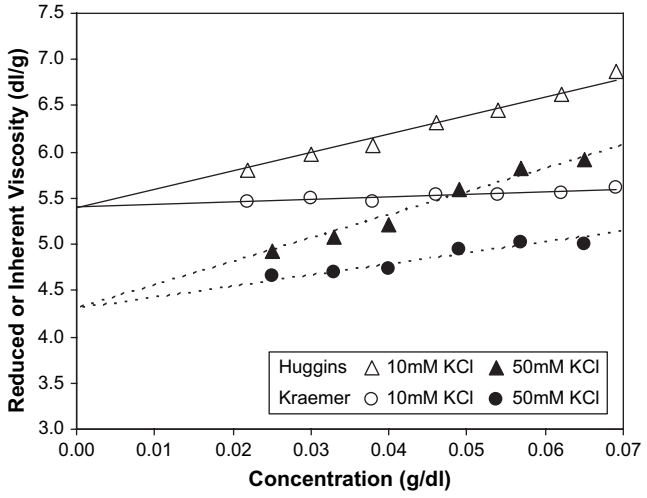

Fig. 2. Reduced and inherent viscosities of model HASE-20-80-2 in 10 and 50 mM salt concentration [KCl]. The solid lines (10 mM KCl) and dotted lines (50 mM KCl) represent the extrapolation of the reduced and inherent viscosity data to zero polymer concentration using Eqs. (3) and (4) to obtain $[\eta]$ and K_h.

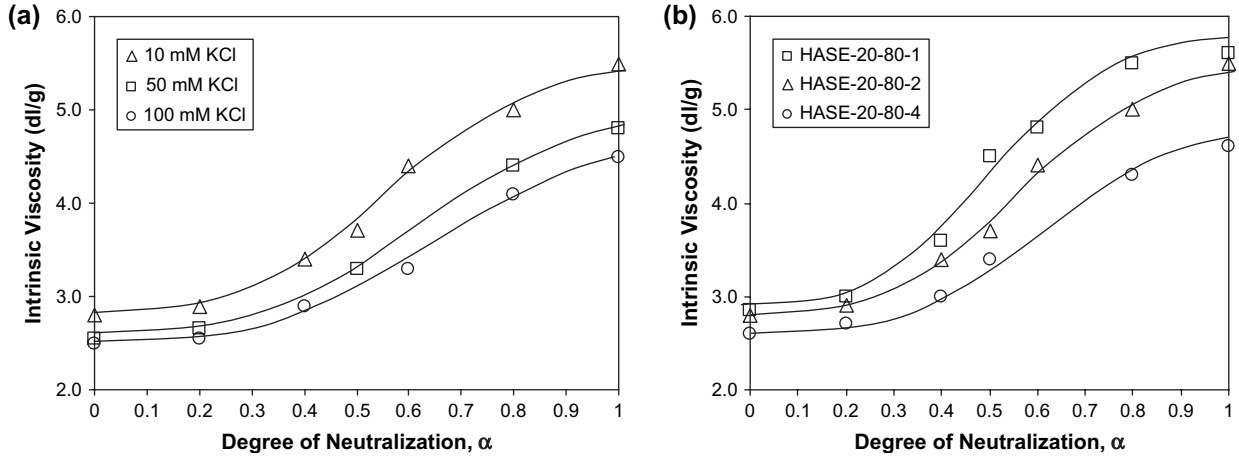

Fig. 3. Intrinsic viscosity, [η], as a function of neutralization degree, α, of: (a) HASE-20-80-2 at three different salt concentrations and (b) microgels with three different cross-linked densities in 10 mM KCl solution.

Fig. 4a shows the relationship between Huggins coefficient, K_h, as a function of α for HASE-20-80-2 microgel in three different salt concentrations, while Fig. 4b describes the relationship between K_h and α for microgels with three different cross-linked densities, i.e. 1, 2 and 4 wt% all prepared in 10 mM KCl solution. When base was added (corresponding to an increasing α) and decreasing salt concentration and microgel cross-linked density, the osmotic pressure of the particle increased and charged shielding effect reduced. The particle–solvent interaction was enhanced due to the exposure of negatively charged carboxylate groups to the solvent environment, which caused K_h to decrease with increasing α and decreasing salt concentrations and cross-linked density as clearly shown in Fig. 4a and b. From the definition of Huggins coefficient, a lower K_h implied that the particle–solvent interaction was enhanced. For microgels with 2 wt% cross-linked density in 10 mM KCl solution, increasing α from 0 to 1 caused K_h to decrease by more than half, i.e. from 2 to 0.7. However K_h increased by almost twice when the salt concentration was increased from 10 to 100 mM KCl for fully neutralized HASE-20-80-2 (Fig. 4a). Similarly, increasing the microgel cross-linked density from 1 to 4 wt% caused K_h of fully neutralized mirogels to increase by two times, i.e. from 0.6 to 1.2 (Fig. 4b).

3.3. Particle–solvent interaction from static light scattering measurement

Static light scattering experiments were conducted to determine the molecular weight, M_w, and second virial coefficient, A_2, of microgels at various α, and at seven different scattering angles. The Zimm plot of HASE-20-80-2 is shown in Fig. 5 at $\alpha = 0$ (Fig. 5a) and $\alpha = 1$ (Fig. 5b).

Results from static light scattering (Fig. 6a and b) clearly showed that before neutralization ($\alpha = 0$), the microgel particles possessed a molecular weight of between 190 and 220×10^6 g/mol and a negative second virial coefficient of $\sim -1.0 \times 10^{-4}$ cm^3 mol/g^2, regardless of salt concentration and cross-linked density. This is due to the seeded emulsion polymerization process employed, where an in-situ seed

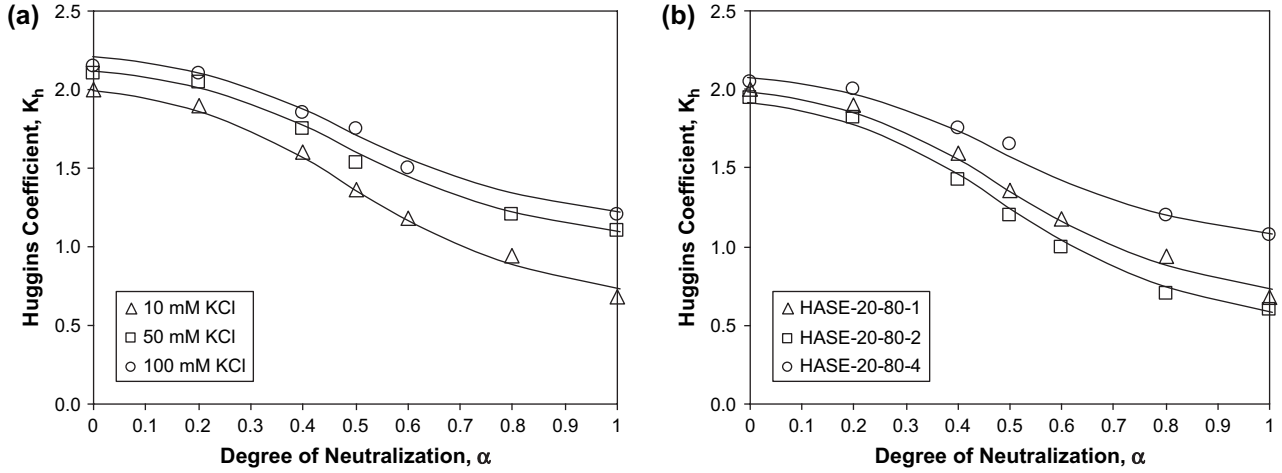

Fig. 4. Dependence of Huggins coefficient, K_h, as a function of neutralization degree, α, of (a) HASE-20-80-2 at three different salt concentrations and (b) microgels with three different cross-linked densities in 10 mM KCl solution.

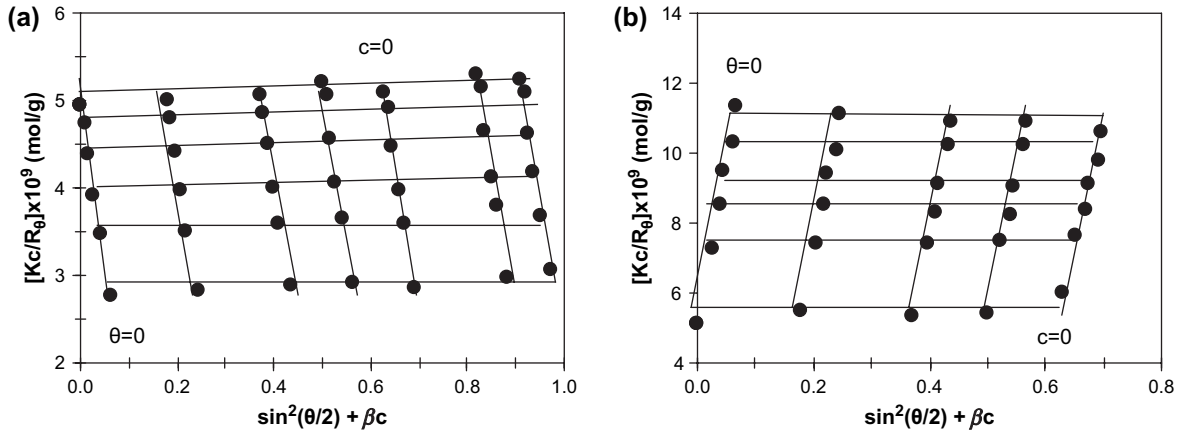

Fig. 5. Zimm plot of HASE-20-80-2 at: (a) $\alpha = 0$ and (b) $\alpha = 1$ in 10 mM KCl at room temperature where the polymer concentration range was from 0.001 to 0.01 mg/ml.

product with approximately similar number of monomer units (hence similar $\overline{M}_w$) was cross-linked to produce a compact particle consisting of many polymer chains. A negative A_2 suggests that the particle–solvent interaction is poor because of the carboxylic acid and ethyl acrylate segments forming a compact insoluble spherical particle.

The $\overline{M}_w$ of the microgels remained unchange at about 200×10^6 g/mol with increasing α, salt concentrations (Fig. 6a) and microgel cross-linked density (Fig. 6b). This demonstrated that no expulsion of polymer chains from the microgel particles occurred during the swelling and deswelling process. We have shown previously that above 1 wt% cross-linked density, microgels with 20 mol% MAA were fully cross-linked to yield an optimal swollen particle [17].

On the other hand, A_2 for microgel HASE-20-80-2 in all three different salt solutions increased with increasing α as shown in Fig. 6a. At low salt concentration of 10 mM KCl, increasing α to 1 caused A_2 of HASE-20-80-2 to increase progressively from 6×10^{-5} to 2.4×10^{-4} cm^3 mol/g^2 as depicted in Fig. 6a. The increase in A_2 upon neutralization suggested that the particle–solvent interaction was enhanced due to the exposure of negatively charged carboxylate groups to the solvent environment when the particle swelled. However, when the salt content was increased to 100 mM KCl, A_2 values for fully neutralized microgels decreased from 2.4×10^{-4} to 1.7×10^{-4} cm^3 mol/g^2 due to poorer polymer–solvent interaction. The reduction in the second virial coefficient indicated that the interaction between charged carboxylate groups and solvent was suppressed by charged shielding from counter-ions. Similarly, increasing the microgel cross-linked density from 1 to 4 wt% caused the A_2 values for fully neutralized microgels to decrease from 2.5×10^{-4} to 2.0×10^{-4} cm^3 mol/g^2 (Fig. 6b). Increasing microgel cross-linked density reduced the exposure of negatively charged

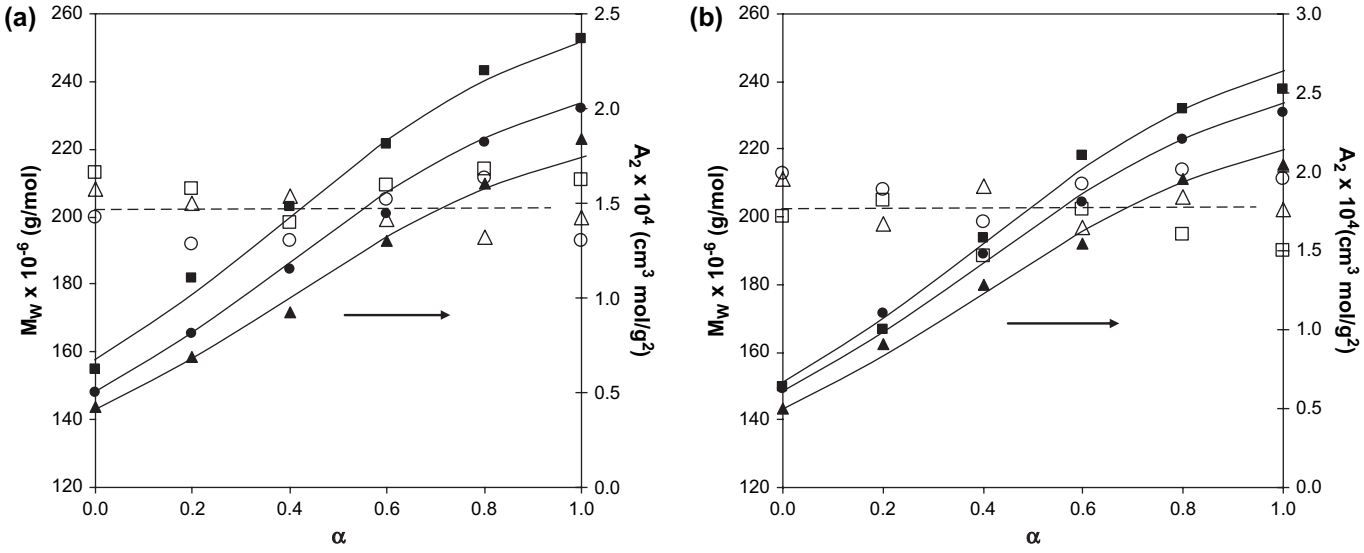

Fig. 6. Molecular weight, $\overline{M}_w$ (open symbols) and second virial coefficient, A_2 (closed symbols) as a function of neutralization degree, α, of: (a) HASE-20-80-2 at three different [KCl] concentrations (mM KCl) (□: 10 mM; ○: 50 mM; △: 100 mM) and (b) microgels with three different cross-linked densities (wt% DAP) in 10 mM KCl solution (□: 1 wt%; ○: 2 wt%; △: 4 wt%). The dotted lines and solid lines demonstrate the trend of the molecular weight and second virial coefficient, respectively.

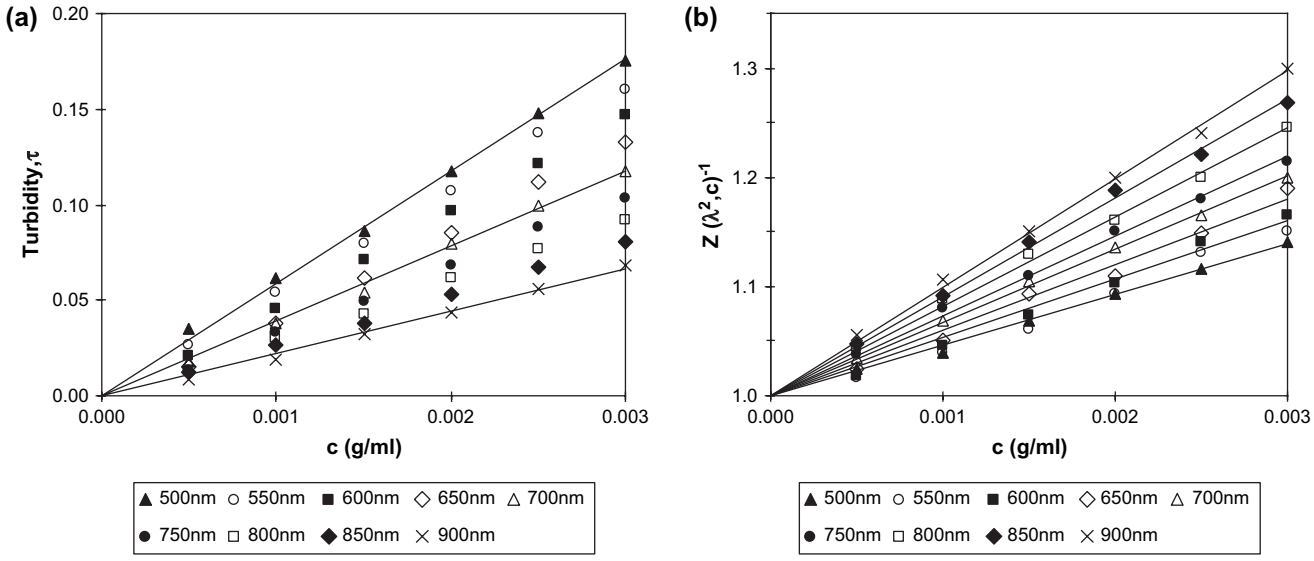

Fig. 7. (a) Turbidity, τ, as a function of wavelength, λ, obtained from UV–visible spectroscopy for six different microgel concentrations of HASE-20-80-4 in 10 mM KCl solution and $\alpha = 1$. (b) Reciprocal integrated structure factor, $Z(\lambda^2,c)^{-1}$, versus the microgel concentration, c, of HASE-20-80-4 to extract the wavelength dependent apparent second virial coefficient, B_{app}, from the slopes of the curves at different wavelengths as suggested by Eq. (7).

carboxylate groups to the solvent environment, thus reducing the interaction between particle and solvent environment.

3.4. Particle–solvent interaction from turbidimetry measurement

As discussed earlier, the particle solvent interaction potential is related to the structural properties of microgels [23–28]. Turbidimetry can be used to study the particle–solvent interaction parameter of dilute and concentrated colloidal suspensions, as this method is practically insensitive to multiple scatterings. Fig. 7a displays the turbidity, τ, as a function of microgel concentration, c obtained from turbidity measurements, for six different microgel concentrations of HASE-20-80-4 in 10 mM KCl solution at $\alpha = 1$. With increasing microgel concentration, the transmitted intensity at a given wavelength decreased and hence the turbidity of the suspension increased as demonstrated in Fig. 7a.

As described in our previous publication, the method of Ballauff and co-workers was employed to extract the contribution of particle–solvent interaction to the structure factor of microgels from the turbidity data [19]. The specific turbidity, τ/c, was plotted as a function of c at fixed wavelength, λ, which permits the intercept $(\tau/c)_{c=0}$, to be extracted. Subsequently, the values of $Z(\lambda^2,c)$ was calculated as prescribed by Eq. (6). To investigate the particle–solvent interaction behavior of our microgels in the low concentration regimes, the reciprocal of the integrated structure factor, $Z(\lambda^2, c)^{-1}$ (Eq. (7))

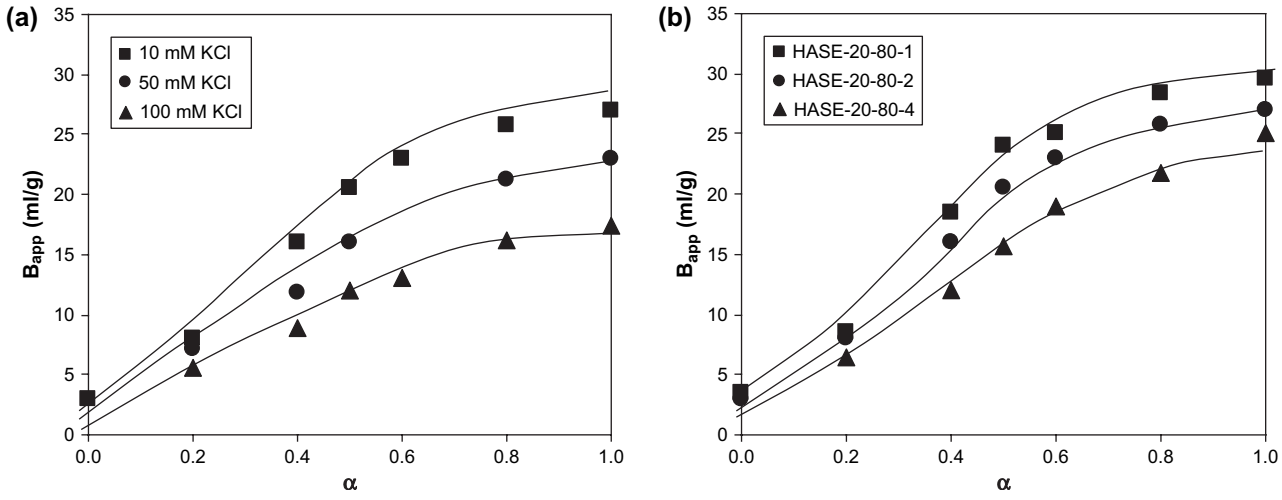

Fig. 8. Relationship between the apparent second virial coefficient, B_{app}, as a function of the neutralization degree, α, of: (a) HASE-20-80-2 at three different [KCl] concentrations (mM KCl) and (b) microgels with three different cross-linked densities (wt% DAP) in 10 mM KCl solution. The solid lines demonstrate the increasing trend of B_{app}.

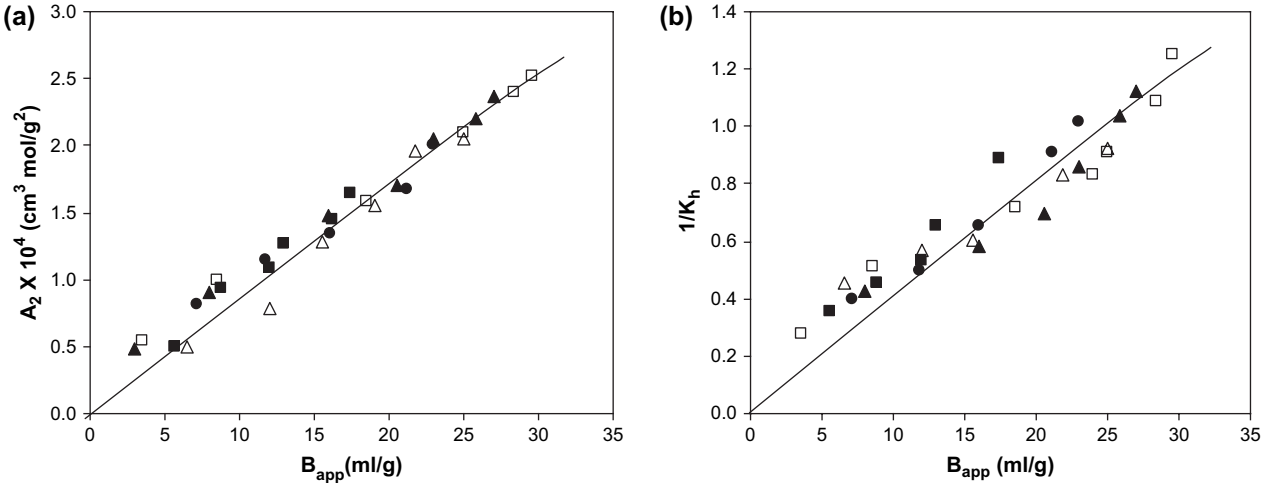

Fig. 9. (a) Second virial coefficient, A_2, as a function of the apparent second virial coefficient, B_{app}, and (b) relationship between inverse of Huggins coefficient, and B_{app} of HASE-20-80-2 at three different [KCl] concentrations (mM KCl) (■: 10 mM; ●: 50 mM; ▲: 100 mM) and HASE-20-80-1 (□) and HASE-20-80-4 (△) both in 10 mM KCl solution.

was plotted as a function of microgel concentration, c (g/ml), in Fig. 7b. The apparent wavelength dependent second virial coefficients, B_{app}, which describes the degree of particle–solvent interaction, were obtained from the slopes of the curves at different wavelengths shown in Fig. 7b as prescribed by Eq. (7).

Fig. 8a and b shows the relationship between the apparent second virial coefficient, B_{app}, as a function of α in three different salt concentrations and three different cross-linked densities, respectively. For all salt concentrations and cross-linked densities, increasing α caused B_{app} to increase by almost ten times at $\alpha = 1$ compared to $\alpha = 0$. This is due to the greater amounts of charged carboxylate groups (COO^-) inside the microgel, which interacts better with the solvent environment, thus improving the interaction between polymer and solvent. However, when the salt concentration was increased from 10 to 100 mM KCl and cross-linked density increased from 1 to 4 wt%, the B_{app} values decreased due to poorer particle–solvent interaction as depicted in Fig. 8a and b, respectively.

3.5. Comparison of the three techniques

As a comparison, the second virial coefficient, A_2, obtained from static light scattering was plotted against the apparent second virial coefficient, B_{app}, obtained from turbidity measurements for the three microgels with different cross-linked densities and in three different salt concentrations (Fig. 9a). For all the microgels, B_{app} increased proportionally to A_2 ($A_2 \propto B_{app}$) and all the data for the three different salt concentrations collapsed onto a single master curve. Both A_2 and B_{app} represent the degree of interaction between polymer and solvent and Fig. 9a confirmed that the relationship between A_2 and B_{app} was in good agreement with theory. Similarly, we examined the relationship between $1/K_h$ obtained from viscometric measurements and B_{app} obtained from turbidity measurements for all the microgel systems. Fig. 9b shows that B_{app} is proportional to $1/K_h$ ($1/K_h \propto B_{app}$) for the three microgels with different cross-linked densities and salt concentrations. All the data collapsed onto a single master curve.

We proposed a scaling relationship between the three parameters (A_2, K_h and B_{app}) described by Eq. (9):

$$\frac{B_{app}}{K_h} \propto \alpha \overline{M}_w A_2 \tag{9}$$

As described previously, Huggins constant, K_h, is dependent on the molecular-weight for polymers that associate easily in solution, by either strong ionic or polar interactions [14]. K_h decreased linearly as molecular weight increased, i.e. $1/K_h \propto M_w$. For high molecular weight microgels ($M_w > 10^5$ g/mol), the second virial coefficient, A_2, was nearly independent of molecular weight [25]. The total scattering intensity and turbidity measurements are complimentary

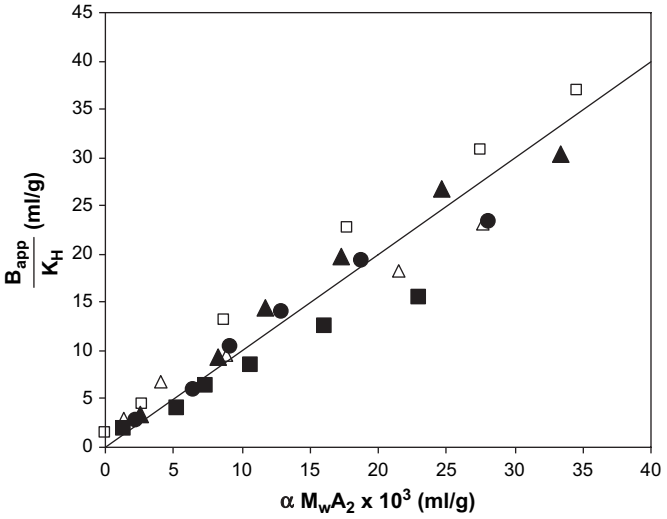

Fig. 10. B_{app}/K_h as a function of HASE-20-80-2 at three different [KCl] concentrations (mM KCl) (■: 10 mM; ●: 50 mM; ▲: 100 mM) and HASE-20-80-1 (□) and HASE-20-80-4 (△) both in 10 mM KCl solution

techniques as shown in the classical Debye equation (Eq. (8)) where $A_2 \propto B_{app}$ [12,31]. Based on our results in Fig. 9 and the above theoretical findings, the empirical equation relating Huggins constant, K_h, apparent second virial coefficient, B_{app}, molecular weight, M_w, second virial coefficient, A_2, and neutralization degree, α, is proposed as given in Eq. (9). From Eq. (9), the B_{app}/K_h data were plotted as a function of $\alpha\overline{M}_w A_2$ for all the three microgels with different cross-linked densities and in three different salt concentrations as depicted in Fig. 10. Excellent agreement was observed where all the data collapsed onto a master curve which confirmed that the data obeyed the scaling expression as shown in Eq. (9).

4. Conclusions

Viscometry, static light scattering and turbidimetric studies were performed to investigate the interaction between pH-responsive microgels and solvent at varying degree of neutralization, α, salt concentrations, and microgel cross-linked densities. Three independent interaction parameters, i.e. Huggins constant, K_h, second virial coefficient, A_2 and apparent second virial coefficient, B_{app}, which describe the degree of particle–solvent interactions, were obtained from these techniques. Based on the theoretical definition of each parameter, we proposed the following scaling relationship, $B_{app}/K_h \propto \alpha\overline{M}_w A_2$. Good agreement was observed where all the data collapsed onto a single master curve. This observation suggested that any of the above techniques can accurately predict the degree of interaction between microgel particle and solvent. It is recommended that turbidimetric technique can be used as it is the simplest among the three techniques.

Acknowledgements

We appreciate the support and enthusiasm of Dow Chemicals in this research collaboration with NTU. The financial support from the Ministry of Education and Singapore-MIT Alliance is acknowledged.

References

[1] Foss AC, Peppas NA. Eur J Pharm Biopharm 2004;57(3):447.
[2] Foss AC, Goto T, Morishita M, Peppas NA. Eur J Pharm Biopharm 2004;57(2):163.
[3] Morris GM, Vincent B, Snowden MJ. J Colloid Interface Sci 1997;190:198.
[4] Beebe DJ, Moore JS, Bauer JM, Yu Q, Liu RH, Devadoss C, et al. Nature 2000;404:588.
[5] Hunter RJ. Foundations of colloid science, vol. 1. Oxford: Clarendon Press; 1991.
[6] Hunter RJ. Foundations of colloid science, vol. 2. Oxford: Clarendon Press; 1991.
[7] Candau F, Ottewill RH. An introduction to polymer colloids. Dordrecht: Kluwer Academic Publishers; 1990;
Krieger IM, Dougherty TJ. Trans Soc Rheol 1959;3:137.
[8] Huglin MB, Rego JM. Macromolecules 1991;24:2556.
[9] Xue W, Huglin MB, Jones TGJ. Eur Polym J 2005;41:239.
[10] Flory PJ. Principles of polymer chemistry. Cornell University Press; 1953 [chapter 13].
[11] Arleth L, Xia X, Hjelm RP, Wu J, Hu Z. J Polym Sci Part B Polym Phys 2005;43:849.
[12] Abed MA, Saxena A, Bohidar HB. Colloids Surf A 2004;233:181.
[13] Abed MA, Bohidar HB. Int J Bio Macromol 2004;34:49.
[14] Choukchou-Braham E, Benabadji I, Mansri A, Francois J. Eur Polym J 2003;39:297.
[15] Tan BH, Tam KC, Lam YC, Tan CB. J Rheol 2004;48:915.
[16] Tan BH, Tam KC, Lam YC, Tan CB. Polymer 2004;45:5515.
[17] Tan BH, Tam KC, Lam YC, Tan CB. Adv Colloid Interface Sci 2005;113:111.
[18] Tan BH, Tam KC, Lam YC, Tan CB. Langmuir 2004;20(26):11380.
[19] Tan BH, Tam KC, Lam YC, Tan CB. Langmuir 2005;21:4283.
[20] Huggins ML. J Am Chem Soc 1942;64:2716.
[21] Kraemer EO. Ind Eng Chem 1938;30:1200.
[22] Dort I. Polymer 1988;29:490.
[23] Zimm BH. J Chem Phys 1948;16:1093.
[24] Zimm BH. J Chem Phys 1948;16:1099.
[25] Berkowitz JB, Yamin M, Fuoss RM. J Polym Sci 1958;28:69.
[26] Apfel U, Grunder R, Ballauff M. Colloid Polym Sci 1994;272:820.
[27] Apfel U, Grunder R, Ballauff M. Langmuir 1995;11:3401.
[28] Weiss A, Potschke D, Ballauff M. Acta Polym 1996;47:333.
[29] Weiss A, Horner KD, Ballauff MJ. Colloid Interface Sci 1999;213:417.
[30] Ramakrishnan S, Fuchs M, Schweizer KS, Zukoski CF. Langmuir 2002;18:1082.
[31] Debye PJ. Appl Phys 1944;15:338.